Isoelectronic Series of Oxygen Deficient Centers in Silica: Experimental Estimation of Homogeneous and Inhomogeneous Spectral Widths

Michele D'Amico,*,†,‡ Fabrizio Messina,† Marco Cannas,† Maurizio Leone,†,‡ and Roberto Boscaino†

Dipartimento di Scienze Fisiche ed Astronomiche, Università degli Studi di Palermo, Via Archirafi 36, I-90123 Palermo, Italy, and Istituto di Biofisica, U.O. di Palermo, Consiglio Nazionale delle Ricerche, Via U. La Malfa 153, I-90146 Palermo, Italy

Received: June 18, 2008; Revised Manuscript Received: September 16, 2008

We report nanosecond time-resolved photoluminescence measurements on the isoelectronic series of oxygen deficient centers in amorphous silica related to silicon, germanium and tin atoms, which are responsible of fluorescence activities at ∼4 eV under excitation at ∼5 eV. The dependence of the first moment of their emission band on time and that of the radiative decay lifetime on emission energy are analyzed within a theoretical model able to describe the effects introduced by disorder on the optical properties of the defects. We obtain separate estimates of the homogeneous and inhomogeneous contributions to the measured emission line width, and we derive homogeneous spectroscopic features of the investigated point defects (Huang−Rhys factor, homogeneous width, oscillator strength, vibrational frequency). The results point to a picture in which an oxygen deficient center localized on a heavier atom features a higher degree of inhomogeneity due to stronger local distortion of the surrounding matrix. For Si, Ge, and Sn related defects, the parameter λ, able to quantify inhomogeneity, is 65, 78, and 90%, respectively.

1. Introduction

Amorphous silicon dioxide (silica) is a wide band gap insulator widely used in present optical and electronic technologies. As a matter of fact, it is the material of choice to fabricate the insulating films incorporated in common metal-oxide-semiconductor (MOS) transistors and optical components to be used in the ultraviolet (UV) spectral range, such as lenses, fibers, and Bragg gratings.[1,2] Since the presence of point defects in SiO_2 significantly compromises the performance of the material in applications, defects in SiO_2 are an important and widely debated technological problem in current literature.

On the other side, the physics of color centers embedded in an amorphous matrix is a fundamental scientific problem which poses several unanswered questions.[3] In a crystal, members of an ensemble of identical defects are virtually indistinguishable from the spectroscopical point of view, since their local environments are identical as well due to translational invariance of the solid. Hence, absorption or photoluminescence (PL) lineshapes, as well as decay lifetimes, are to be considered in this case as homogeneous properties of the defects. On the other hand, defects in an amorphous solid are supposedly characterized by statistical distributions of the spectroscopic properties, since the disorder of the matrix gives rise to site-to-site differences among the environments experienced by the single centers. For this reason, it is generally assumed that the lineshapes of their optical bands feature an inhomogeneous broadening,[1,2,4] so that the overall spectroscopic properties of an "amorphous defect" are determined by the concurrence of homogeneous and inhomogeneous effects.

While this general interpretation scheme is widely accepted in literature, no general approach is currently available to separate the homogeneous and inhomogeneous contributions to the experimentally observed line width of an absorption or PL band. Moreover, almost nothing is known on the effect of inhomogeneity on the decay properties of a defect. The homogeneous absorption line width is due to electron−phonon interaction, and is determined by basic physical properties of the defect, namely the Huang−Rhys factors and the phonon vibrational frequencies.[1,2] In the past, many techniques were used to attempt its estimation in several heterogeneous systems: exciton resonant luminescence, resonant second harmonic scattering, femtosecond photon echo, spectral hole burning.[5−8] This last technique is particularly interesting also for its technological implications, namely the promising feature of writing information bits as homogeneous "holes" in a sufficiently broad inhomogeneous optical band, thus creating solid state optical memories with very high bit density.[2,4]

In a recent paper,[9] we have proposed a new experimental approach to this problem, which allows to estimate the inhomogeneous and homogeneous linewidths of a defect based on studying the variations of the radiative decay lifetime within an inhomogeneously broadened emission band. Our aim here is to apply this technique to a particular kind of point defect in silica, the so-named oxygen deficient center of the second type, shortly ODC(II). The ODC(II) exists as an intrinsic defect or in two extrinsic varieties related to the impurity content. Its mostly accepted structural model consists in a 2-fold coordinated atom ($=X^{\bullet\bullet}$),[10−12] where X can be either a Si (Si-ODC(II)), a Ge (Ge-ODC(II)), or a Sn (Sn-ODC(II)) atom. However, the structure of Si-ODC(II) is still debated at the moment,[1,13,14] as it has been proposed an alternative model of the defect as a neutral oxygen vacancy between two silicon atoms ($\equiv Si-Si\equiv$).[15,16] Due to their isoelectronic outer valence shell ($ns^2\,np^2$ with $n = 3-5$) the defects belonging to this group feature similar optical

* To whom correspondence should be addressed. E-mail: damico@fisica.unipa.it.
† Università degli Studi di Palermo.
‡ Consiglio Nazionale delle Ricerche.

10.1021/jp805372u CCC: $40.75
Published on Web 10/31/2008

activities (e.g., emission and absorption peaks and singlet decay lifetimes).[13] A more interesting feature of the ODCs(II) is that some of their spectroscopic parameters (e.g., nonradiative decay rates and triplet decay lifetimes) regularly vary along the isoelectronic series, according to the expected effect of introducing a heavier central atom along the Si−Ge−Sn series.[13,17] Indeed, this property was used as an important clue to prove a common structural model of the three defects. Regarding the optical activities, ODC(II) are responsible of intense signals in the vis−UV range: Si-ODC(II) mainly gives rise to a broad nearly Gaussian optical absorption (OA) band centered at ∼5.0 eV due to the transition between the ground singlet (S_0) and the first excited singlet (S_1) state. This absorption excites a fast (lifetime in the ns range) emission band centered at ∼4.4 eV, due to the inverse $S_1 \rightarrow S_0$ transition.[12,13] At $T > 300$ K, it is possible also to populate from S_1 the first excited triplet state (T_1) by the nonradiative intersystem crossing process (ISC). In these conditions one observes an additional slow (ms) decaying emission centered at ∼2.7 eV, due to the $T_1 \rightarrow S_0$ transition. The corresponding bands for Ge-ODC(II) are centered at ∼5.1 eV (OA), the fluorescence at ∼4.3 eV and phosphorescence at ∼3.1 eV (active at $T > 100$ K).[13,18] Finally, for Sn-ODC(II) they are centered at ∼4.9, ∼4.2, and ∼3.1 eV (active at $T >$ 50 K) respectively.[19] The PL signal of ODC(II) is characteristic of the amorphous phase of silicon dioxide, where it is usually observed both in as-grown materials or after irradiation. In contrast, it has never been observed in crystalline SiO_2,[13] so that ODC(II) represent an interesting model system to perform experiments aimed at investigating the peculiar properties of defects in disordered materials.

Previous optical measurements on the intrinsic and extrinsic ODC(II) bands have already suggested that ODC(II) are significantly affected by inhomogeneous effects.[19−22] However, no quantitative estimate exists of their degree of inhomogeneity. Time-resolved PL measurements reported here clearly evidence inhomogeneous effects affecting the decay properties of these defects. Furthermore, they provide for the first time the possibility of estimating the inhomogeneous and homogeneous widths of ODC(II) emission bands, and analyze how they depend on the nature of the central atom.

2. Experimental Methods

We report measurements performed on three samples chosen because they contain Si-ODC(II), Ge-ODC(II), and Sn-ODC(II) defects, respectively. The first sample is a synthetic silica specimen (commercial name: Suprasil300), hereafter named S300, with a nominal concentration of impurities <1 ppm in weight. The second one is a fused silica sample (commercial name: Infrasil301), hereafter named I301, manufactured by fusion and quenching of natural quartz, with typical concentration of impurities ∼20 ppm in weight. In particular, as-grown I301 features a ∼1 ppm concentration of Ge impurities, due to contamination of the quartz from which the material was produced. These two samples were provided by Heraeus Quartzglas[23] and were 5 × 5 × 1 mm^3 sized. The last silica sample is doped with 2000 ppm of Sn atoms, hereafter named Sn-doped silica, prepared by the sol−gel method as described in ref 24 and rod shaped with a diameter of 4 mm and thickness of 1.4 mm.

PL measurements were done in a standard back-scattering geometry, under excitation by a pulsed laser (Vibrant OPOTEK: pulsewidth of 5 ns, repetition rate of 10 Hz, energy density per pulse of 0.30 ± 0.02 mJ/cm^2) tunable in the UV−visible range. The luminescence emitted by the sample was dispersed by a spectrograph (SpectraPro 2300i, PI Acton, 300 mm focal length) equipped by a 300 grooves/mm grating (blaze at 500 nm, bandwidth = 3 nm), and detected by an air-cooled intensified CCD (Charge-Coupled Device PIMAX, PI Acton). The detection system can be triggered so as to acquire the emitted light only in a given temporal window defined by its width (t_W) and by its delay t from the laser pulse. Our experimental setup features an acquisition deadtime related to the falling front of laser pulse. In the following, the origin ($t = 0$) of the time scale is accordingly defined as the time of the first possible measurement, corresponding to about ∼2 ns after the instant of arrival of laser peak intensity. All PL signals were corrected for spectrograph dispersion and instrumental response. All measurements reported here were performed on silica samples kept at cryogenic temperature (10 K) in high vacuum (∼10^{-6} mbar) within a He flow cryostat (Optistat CF-V, OXFORD Inst.).

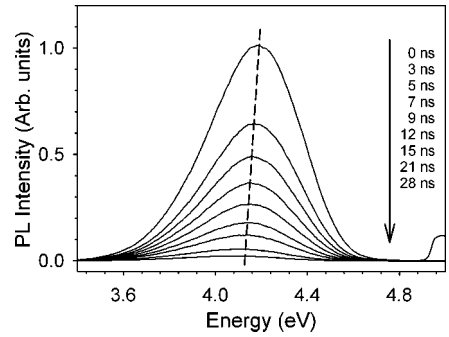

Figure 1. Lineshape of Sn-ODC(II) PL activity as excited by 5.00 eV laser. Different spectra measured at different time delays from laser pulse are shown. The dashed line follows the PL peak position for eye-guiding purposes.

3. Results

In Figure 1, we show a typical time-resolved measurement of the PL activity of Sn-ODC(II) in the Sn-doped silica sample.

The measurement was performed under laser excitation at 248 nm (5.00 eV), corresponding to the peak absorption wavelength of the defect at cryogenic temperature. The PL signal $L(E, t)$ was monitored by performing 120 acquisitions with the same integration time $t_W = 0.5$ ns but at different delays t, going from 0 to 60 ns. The dashed line reported in Figure 1 follows the peak position of PL band as a function of the delay time from the laser pulse: there is a clear evidence of a progressive change of the observed PL line shape, whose peak moves from 4.2 eV at $t = 0$ ns to 4.1 eV at $t = 28$ ns. In Figure 2c, we report the signal acquired for $t = 0$, corresponding to the most intense spectrum in Figure 1. The PL band of Sn-ODC(II), as acquired immediately after the end of the laser pulse, is peaked at ∼4.2 eV and features a 0.48 eV width (Full Width at Half Maximum, fwhm).

Analogous time-resolved measurements were carried out on the PL activity of Si-ODC(II) defects in the S300 sample using a 248 nm (5.00 eV) excitation wavelength. The decay was monitored varying t from 0 to 20 ns and with $t_W = 0.5$ ns. We report in Figure 2a the spectrum acquired for $t = 0$: the PL band of Si-ODC(II), as acquired immediately after the end of the laser pulse, is peaked at ∼4.4 eV and features a 0.35 eV fwhm.

Finally, the I301 sample was excited at 240 nm (5.17 eV) and the luminescence of Ge-ODC(II) was monitored varying t from 0 to 60 ns with $t_W = 1$ ns. As shown in Figure 2b the PL signal detected in this sample immediately after the end of the laser pulse is peaked at ∼4.3 eV and features a 0.45 eV fwhm.

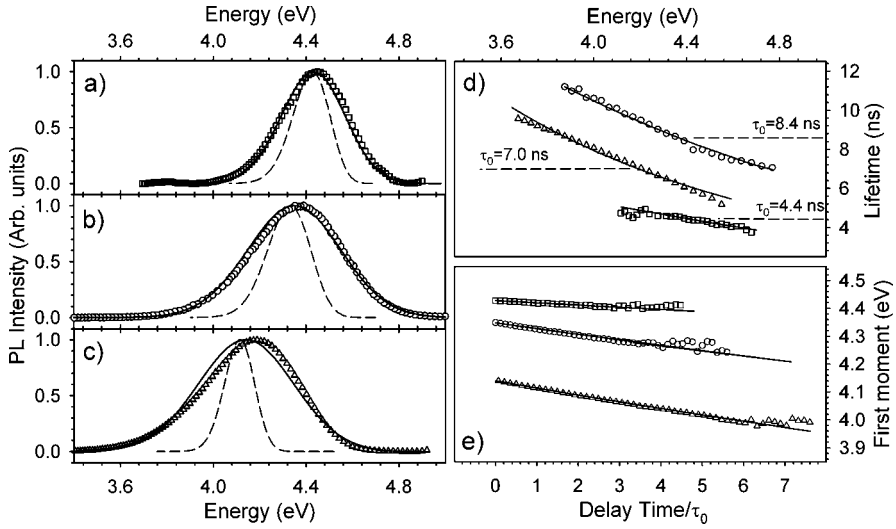

Figure 2. Low temperature luminescence line shape of Si-ODC(II) (panel a), Ge-ODC(II) (panel b), and Sn-ODC(II) (panel c) at $t = 0$. Panel d: decay lifetime as measured at different emission energies within the emission band as measured for Si-ODC(II) (squares), Ge-ODC(II) (circles) and Sn-ODC(II) (triangles). Panel e: first moment of the emission band as a function of time. The continuous lines are the result of the fitting procedure by the theoretical model in ref 9; the dashed lines in panels a−c are the homogeneous Poissonian line shapes (see discussion).

For each of the three activities (Si-ODC(II), Ge-ODC(II), and Sn-ODC(II)), we calculated the PL decay lifetime $\tau(E)$ at different emission energies E. At the chosen measurement temperature, the decay kinetics of all the three activities result to be single-exponential due to quenching of the nonradiative decay channels.[12,13,19,25] As a consequence, the radiative lifetimes were obtained by fitting with a single exponential function (1) data at several values of E.[30]

$$I(E,t) = I(E,0)\mathrm{e}^{-t/\tau(E)} \quad (1)$$

In Figure 2d, we report so-calculated lifetimes $\tau(E)$ and we observe that all PL activities in silica feature a dispersion of the radiative lifetime as a function of the emission energy: the lifetime goes from ∼4 to ∼5 ns for the Si-ODC(II), from ∼7 to ∼11 ns for the Ge-ODC(II) and from ∼5 to ∼9 ns for the Sn-ODC(II). Also, we calculated by numerical integration from time-resolved spectra $L(E, t)$ (as in Figure 1 for Sn doped sample) the time dependence $M_1(t)$ of the first moment of the luminescence bands. The temporal behavior of first moments for the three silica samples are reported in Figure 2e, where the horizontal axis represents the time delay t from the laser pulse in units of the central lifetime τ_0 observed at the peak emission energy (indicated in Figure 2d). We observe that all PL activities in silica feature an approximately linear decrease of the first moment $M_1(t)$ in time, with a negative slope increasing with the atomic weight of ODC(II) defects. The two results are directly connected: indeed, the dependence of the lifetime from the spectral position within the emission band corresponds to (and can be alternatively understood as) a progressive shift of first momentum of PL bands; moreover the different dependencies of τ from emission energy of Figure 2d correspond, as expected, to different slopes in Figure 2e. Summing up, these experimental findings are the ultimate reasons that bring about the observed dispersion of the emission line shape as observed representatively in Figure 1 for the Sn doped sample.

4. Discussion

We have recently proposed a theoretical model that allows to interpret the behavior of ODC(II) in panels d and e of Figure 2, namely the distribution of lifetimes measured at different emission energies and the correspondent red-shift of the first moment of the singlet PL band as a function of delay time.[9] The model explains both features in terms of a Gaussian statistical distribution of a single homogeneous parameter of the defect: the zero phonon (ZPL) energy E_0, i.e., the energy difference between the ground and the first excited electronic states of the center, both in the ground vibrational sublevel. Every other spectroscopic feature of the defect (the homogeneous half-width σ_{ho}, the oscillator strength f, the half Stokes shift S) is assumed as undistributed. Furthermore, the defect is assumed to be coupled to a single vibrational mode which frequency is thought as an opportunely defined "mean" frequency of all modes coupled to the electronic transition. Coupling with a single frequency should be regarded as a simplified, though effective, representation of the much more complicated picture of electron−phonon coupling. Also, it is worth noting that in this scheme one cannot distinguish between a single mode with a strong coupling and several degenerate modes with weaker coupling. For the present purposes, this statistical distribution of E_0 is equivalent to a distribution of the peak PL emission energy E_{e}, and physically represents the existence of different environments which accommodate the defects at different sites of the amorphous matrix.[31] For further details we refer to the original paper.[9]

On these basis, one can write a quantitative expression of the PL emitted by the ensemble of color centers in the amorphous solid[9]

$$L_{\mathrm{s}}(E,t|\widehat{E_{\mathrm{e}}},\sigma_{\mathrm{in}},\sigma_{\mathrm{ho}},f) \propto \int \left[E^3 P(E|E_{\mathrm{e}},\sigma_{\mathrm{ho}})\mathrm{e}^{-t/\tau(E_{\mathrm{e}},\sigma_{\mathrm{ho}},f)}\right]\mathrm{e}^{-(E_{\mathrm{e}}-\widehat{E_{\mathrm{e}}})^2/2\sigma_{\mathrm{in}}^2} \times \mathrm{d}E_{\mathrm{e}} \quad (2)$$

Eq. 2 expresses the overall emission signal $L_s(E, t)$ measured at time t at the spectral position E. It is obtained by convolution of a Gaussian distribution of E_e, whose half-width σ_{in} represents the inhomogeneous line width of the ensemble of defects, with a homogeneous term (within squared parentheses) representing the PL of a defect emitting at a given value of E_e and with (undistributed) homogeneous half-width σ_{ho}: the spectral shape of the homogeneous term is $E^3P(E|E_{em}, \sigma_{ho})$, the P function being a Poissonian with first moment E_e and second moment σ_{ho}, and its radiative lifetime is given by the Forster's equation:[26]

TABLE 1: Upper Section: Best Fitting Parameters Obtained by Our Theoretical Model for the Investigated PL Activities and Lower Section: Values of λ, σ_{tot} (Calculated by $\sigma_{tot}^2 = \sigma_{in}^2 + \sigma_{ho}^2$), $\hbar\omega_p$ and H, as Calculated from Best Fitting Parameters

	$\widehat{E}_e$ [eV]	σ_{in} [meV]	σ_{ho} [meV]	f
Si	4.42 ± 0.05	110 ± 10	80 ± 10	0.134 ± 0.019
Ge	4.32 ± 0.05	177 ± 10	93 ± 12	0.073 ± 0.010
Sn	4.11 ± 0.10	195 ± 10	65 ± 10	0.104 ± 0.014
	λ (%)	σ_{tot} [meV]	$\hbar\omega_p$ [meV]	H
Si	65 ± 4	136 ± 10	24 ± 4	11 ± 4
Ge	78 ± 5	200 ± 10	23 ± 6	17 ± 5
Sn	90 ± 5	206 ± 10	10 ± 4	40 ± 10

$$1/\tau(E_e, \sigma_{ho}, f) = \frac{2e^2n^2}{m_e c^3 \hbar^2} f \int P(E|E_e, \sigma_{ho}) E^3 \, dE \qquad (3)$$

where f is the oscillator strength of the defect, and n is the refractive index of silica.[32] Equation 3 basically arises from Einstein's relation for spontaneous emission integrated on the PL line shape. Summing up, one can numerically integrate eq 2 in order to simulate the time-resolved PL spectra, $L_s(E, t)$, as a function of the four parameters $\hat{E}_e$, σ_{in}, σ_{ho}, and f. From $L_s(E, t)$ one can then easily calculate the decay lifetime $\tau_s(E)$ and the kinetics $M_{1s}(t)$ of the first moment, by using the same procedure applied to the experimental data $L(E, t)$.

Equation 3 implies that defects with different emission positions E_e within the Gaussian distribution should decay with different lifetimes. In this sense, it immediately allows to understand data in Figure 2 on a qualitative basis, if we suppose the PL band of ODC(II) as arising from the inhomogeneous overlap of bands peaked at different energies, statistically distributed within the defect population. Also, data in Figure 2 suggest that the degree of inhomogeneity increases while moving along the Si−Ge−Sn series. In fact, both the slope of $\tau(E)$ (Figure 2d) and that of $M_1(t)$ (Figure 2e) grow with increasing atomic weight of the central atom, thus suggesting the occurrence of progressively stronger inhomogeneous effects.

This argument can be made quantitative by fitting experimental data, for each of the investigated PL activities, with our model (eq 2) in order to estimate σ_{in} and σ_{ho}. Specifically, we have determined by least-squares optimization the best values of the parameters ($\hat{E}_e$, σ_{in}, σ_{ho}, and f) that produce a set of three theoretical curves simultaneously fitting the PL shape at $t = 0$ (Figure 2a−c), the dispersion of the decay lifetimes (Figure 2d) and the kinetics of the first moment (Figure 2e). The continuous lines in Figure 2 represent the results of our fitting procedure. It is worth noting the goodness of the fit obtained by using only four free parameters considering the contemporaneously minimization on spectral and temporal data. Only for the line shape at $t = 0$ of Sn-ODC(II) the fitting curve does not reproduce well the experimental data: this could be due to the presence of another spurious PL signal at lower energy which apparently enlarges the band, or to the partial failure for this defect of the approximations inherent in our model, e.g., more than one homogeneous parameter to be distributed. However, the behavior of first moment and lifetime dispersion are still well reproduced by the theoretical model; hence, we consider the numerical results to be reliable also in this case. In Figure 2a−c we also show, with dashed line, the Poissonian homogeneous line shape of half-width σ_{ho} as obtained by our fit procedure for all investigated activities.

The upper part of Table 1 resumes the best fit parameters obtained for all investigated PL activities. We calculate the parameter $\lambda = \sigma_{in}^2/\sigma_{tot}^2$ which estimates the degree of inhomogeneity. The high values (>65%) of λ show that inhomogeneous effects strongly condition the optical properties of all the ODC(II) defects in silica, σ_{in} being the main contribution to the total width for all the centers. In a sense, this could be expected a priori for a point defect found exclusively in the amorphous phase of SiO_2. On the other hand, it is worth noting that the degree of inhomogeneity is remarkably high, particularly for Sn-ODC(II). For this latter defect, the order of magnitude of the site-to-site fluctuations of the emission peak position results to be as large as $\sigma_{in} \sim 0.2$ eV. The degree of inhomogeneity systematically varies along the isoelectronic series: the value of λ of extrinsic Sn-ODC(II) defects (Sn-doped sample) is higher than that of Ge-ODC(II) extrinsic centers (I301 sample), which is in turn higher than Si-ODC(II) intrinsic defects (S300 sample). These variations of λ are mainly due to the growth of σ_{in} with atomic weight, since variations of σ_{ho} are weaker. This trend can be tentatively interpreted as follows: Ge and Sn impurities are isoelectronic to Si atoms and thus able to be accommodated in substitutional positions. Nonetheless, the distortion they cause to the matrix presumably extends over a larger surrounding volume than a single SiO_2 tetrahedra due to their being bigger and heavier than their intrinsic counterpart. A bigger volume affected by the presence of the defect is expected to result in a higher sensitivity to site-to-site structural fluctuations, which eventually causes stronger fluctuations of E_e. These considerations based on the experimental results reported here are at variance with previous ones based on computational findings in ref 27 where it was argued that heavier Ge and Sn atoms are much less sensitive to the details of local geometry. The results reported here complete the characterization of the isoelectronic series of oxygen deficient centers in silica, by yielding information about their inhomogeneous properties, which adds to existing knowledge founded on traditional spectroscopic investigation.

Other two parameters of interest can be calculated from σ_{ho}: the vibrational frequency $\hbar\omega_p = \sigma_{ho}^2/S$ and the Huang−Rhys factor $H = S^2/\sigma_{ho}^2$. In these expressions, the parameter S represents the half Stokes shift, estimated experimentally by measuring the half-difference between the spectral positions of the excitation energy and emission peaks. S results to be: 0.27, 0.38, and 0.41 eV, in Si, Ge and Sn-ODC(II) respectively. Based on these values of S, we calculate $\hbar\omega_p$ and H, reported in the lower part of Table 1. The vibrational frequencies found here for ODC(II) defects show that all of them are preferentially coupled with very low frequency vibrational modes, accordingly with previous experimental and computational results.[19,28,29] Albeit the relatively high uncertainty on $\hbar\omega_p$ as determined by the fitting procedure, data show a decreasing trend while going from the lightest to the heavier ODC(II). Qualitatively, this is to be expected if one roughly assumes that the variations in the force constant of the vibration are negligible from Si to Sn: indeed, the frequency of a mode highly localized on the central atom should in this case be inversely proportional to the square of its mass. It is possible to object that the lower $\hbar\omega_p$ frequency obtained for Sn-ODC(II) could be affected by the worse fitting result obtained on its PL line shape; on the other side, it is worth stressing that the above-discussed results on heterogeneity are poorly affected by this fact, as they mainly depend on the well fitted slope of the first momentum and lifetime dispersion curves.

Finally, the values of the oscillator strength found here, are in excellent agreement with those reported in a review paper about oxygen deficiency centers in silica:[13] 0.03−0.07 for Ge-ODC(II) and 0.15 for Si-ODC(II).

5. Conclusions

We studied by time-resolved luminescence the defects belonging to the isoelectronic series of oxygen deficient centers in amorphous silicon dioxide. The dispersion of the emission line shape was used as a probe to quantitatively evaluate the influence of inhomogeneous effects on the optical properties of the defects. We provided for Si-ODC(II), Ge-ODC(II), and Sn-ODC(II) an estimate of the inhomogeneous and homogeneous widths, on the grounds of a theoretical model that satisfactorily reproduces all experimental data based on two main simple assumptions: homogeneous optical properties governed by coupling with a single "mean" vibrational mode, and a Gaussian distribution of the ZPL energy accounting for structural heterogeneity. The degree of inhomogeneity of the defects turns out to grow regularly with the atomic weight of the central atom, while the variations of the homogeneous properties are weaker. Along with the homogeneous width, we estimated also the other homogeneous parameters of oxygen deficient centers: oscillator strength, Huang−Rhys factor and mean vibrational frequency of the electron−phonon interaction.

Acknowledgment. We acknowledge financial support received from project "POR Regione Sicilia - Misura 3.15 - Sottoazione C". We are grateful to LAMP research group (http://www.fisica.unipa.it/amorphous/) for support and enlightening discussions. The authors would like to thank G. Lapis and G. Napoli for assistance in cryogenic sessions.

References and Notes

(1) *Defects in SiO_2 and Related Dielectrics: Science and Technology*; Pacchioni, G., Skuja, L., Griscom, D. L., Eds.; Kluwer Academic Publishers: USA, 2000.

(2) *Silicon-based Materials and Devices*; Nalwa, H. S., Ed.; Academic Press: San Diego, CA., 2001.

(3) Stoneham, A. M. *Theory of Defects in Solids*; Oxford: New York, 1975; vol. *1*.

(4) *Persistent Spectral Hole-Burning: Science and Applications*; Moerner, W., Ed.; Springer-Verlag: New York, 1988.

(5) Itoh, T.; Furumiya, M. *J. Lumin.* **1991**, *48−49*, 704.

(6) Kuroda, T.; Matsushita, S.; Minami, F.; Inoue, K.; Baranov, A. V. *Phys. Rev. B* **1997**, *55*, R16041−R16044.

(7) Mittleman, D. M.; Schoenlein, R. W.; Shiang, J. J.; Colvin, V. L.; Alivisatos, A. P.; Shank, C. V. *Phys. Rev. B* **1994**, *49*, 14435–14447.

(8) Woggon, U.; Gaponenko, S.; Langbein, W.; Uhrig, A.; Klingshirn, C. *Phys. Rev. B* **1993**, *47*, 3684–3689.

(9) D'Amico, M.; Messina, F.; Cannas, M.; Leone, M.; Boscaino, R. *Phys. Rev. B* **2008**, *78*, 014203.

(10) Skuja, L.; Streletsky, A. N.; Pakovich, A. B. *Solid State Commun.* **1984**, *50*, 1069.

(11) Nishikawa, H.; Shiroyama, T.; Nakamura, R.; Ohki, Y.; Nagasawa, K.; Hama, Y. *Phys. Rev. B* **1992**, *45*, 586.

(12) Skuja, L. *J. Non-Cryst. Solids* **1994**, *179*, 51.

(13) Skuja, L. *J. Non-Cryst. Solids* **1998**, *239*, 16.

(14) Zatsepin, A.; Kortov, V. S.; Fitting, H.-J. *J. Non-Cryst. Solids* **2005**, *351*, 869.

(15) Jones, C.; Embree, D. *J. Appl. Phys.* **1976**, *47*, 5365.

(16) Imai, H.; Arai, K.; Imagawa, H.; Hosono, H.; Abe, Y. *Phys. Rev. B* **1988**, *38*, 12772.

(17) Skuja, L. *J. Non-Cryst. Solids* **1992**, *149*, 77.

(18) Agnello, S.; Boscaino, R.; Cannas, M.; Gelardi, F. M.; Leone, M. *Phys. Rev. B* **2000**, *61*, 1946.

(19) Cannizzo, A.; Leone, M.; Boscaino, R.; Paleari, A.; Chiodini, N.; Grandi, S.; Mustarelli, P. *J. Non-Cryst. Solids* **2006**, *352*, 2082.

(20) Leone, M.; Agnello, S.; Boscaino, R.; Cannas, M.; Gelardi, F. M. *Phys. Rev. B* **1999**, *60*, 11475–11481.

(21) Cannizzo, A.; Agnello, S.; Boscaino, R.; Cannas, M.; Gelardi, F. M.; Grandi, S.; Leone, M. *J. Phys. Chem. Solids* **2003**, *64*, 2437.

(22) Cannizzo, A.; Leone, M. *Phil. Mag.* **2004**, *84*, 1651.

(23) Quartzglas, H. Hanau, Germany, catalog POL-0/102/E

(24) Chiodini, N.; Meinardi, F.; Morazzoni, F.; Padovani, A.; Paleari, J.; Scotti, R.; Spinolo, G. *J. Mater. Chem.* **2001**, *11*, 926.

(25) Agnello, S.; Boscaino, R.; Cannas, M.; Cannizzo, A.; Gelardi, F. M.; Grandi, S.; Leone, M. *Phys. Rev. B* **2003**, *68*, 165201.

(26) Förster, T. Fluoreszenz Organischer Verbindungen, Vandenhoeck und Ruprecht, Göttinen 1951, 158.

(27) Pacchioni, G.; Ferrario, R. *Phys. Rev. B* **1998**, *58*, 6090.

(28) Galeener, F. L.; Leadbetter, A. J.; Stringfellow, M. W. *Phys. Rev. B* **1983**, *27*, 1052–1078.

(29) Umari, P.; Gonze, X.; Pasquarello, A. *Phys. Rev. Lett.* **2003**, *90*, 027401.

(30) Moreover, the single exponential character of the decays avoids any problem with the experimental deadtime and the consequent choice of the zero of the time scale.

(31) E_e is related to E_0 by $E_e = E_0 - S$. Since S is supposedly undistributed, a Gaussian distribution of E_0 is equivalent to a Gaussian distribution of E_e, shifted by S and with the same width.

(32) In writing eq 3, we have neglected the "effective field correction" term, which can be argued to be close to unity in silica within the investigated spectral range. We also neglect the slight energy dependence of the refraction index n which we assume for silica to be 1.5.

JP805372U